Proton-detected Multidimensional Solid-State NMR enables Precise Characterization of Vanadium Surface Species at Natural Abundance

Deni Mance, Aleix Comas-Vives, Christophe Copéret**

Department of Chemistry and Applied Biosciences, ETH Zürich, Vladimir-Prelog Weg 1-5, CH-8093 Zürich, Switzerland

AUTHOR INFORMATION

Corresponding Author

*Email: mance@inorg.chem.ethz.ch.

*Email: ccoperet@ethz.ch

ABSTRACT

Heterogeneous catalysts fulfill vital roles in industrial process, however due to the nature of the catalytic surfaces typically containing either a low abundance of active sites and being amorphous in nature leads difficulties when attempting to study the structure of the active sites. In this work we show how making use of fast MAS ssNMR probes allows to efficiently detect well resolved ^{1}H detected spectra of heterogeneous catalysts. This approach was applied to study the structure of surface species resulting from the grafting of $VO(OiPr)_3$ onto a partially dehydroxylated silica using the surface organometallic chemistry approach. The use of the ^{1}H sensitivity enabled to detect various hetero- and homo-nuclear correlation spectra in order to study the structure of this system and to resolve the structure of the grafted vanadium complex. More specifically, $VO(OiPr)_3$ grafts through both protonolysis and opening of siloxane bridges to generate a bis-grafted species, in contrast to most other alkoxides.

TOC GRAPHICS

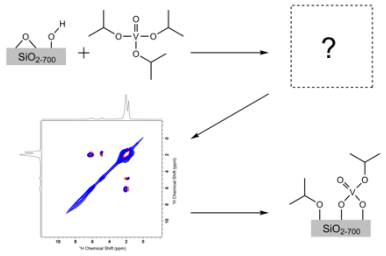

KEYWORDS Solid-State NMR, Heterogeneous Catalysis, proton detection, Surface Organometallic Chemistry

Catalytic processes are the core of modern chemical industry and fulfil various vital roles from solving environmental concerns to developing more sustainable processes.[1–3] In view of further improving these processes, major efforts have concentrated on understanding the structure of catalytically active sites with the ultimate goal to rationally design catalyst. However, gaining molecular level information about active site structure is not straightforward especially for heterogeneous catalysts,[4–7] due to the small amount of active sites and the difficulty to selectively probe surface structures. This is the reason why typically little is known about the active-site or structural changes that occur before and after catalysis. While NMR would be a method of choice to probe the structure of surface sites due to being a non-destructive technique capable of investigated the smallest structural changes without any modifications to the sample and in addition having tools to assess the surface sites specifically by employing Cross-Polarization and Dynamic Nuclear Polarization (DNP) methods[8–10], it particularly suffers from its inherent low sensitivity and in the specific case of quadrupolar nuclei may suffer from significant line broadening. Dynamic Nuclear Polarization (DNP) can be a method of choice to alleviate the sensitivity problem encountered in NMR and has demonstrated promising results on a multitude of systems, but it is currently mostly applied to spin ½ nuclei with limited and often times varying success with quadrupolar nuclei or complex systems[10–17]. Another issue that may arise with this method is the incompatibility of the radical or solvent required for DNP measurements[12] with the catalyst; such an issue can greatly compromise the acquired data and lead to a misguided interpretation of the spectra. The incorporation of isotopically enriched nuclei is therefore strongly desired in order to overcome some of these issues, though not universally practical due to complicating synthesis and not cost effective depending on the necessary quantities. An alternative

method to remedy the sensitivity issue and make studying such systems more accessible would be the use of multidimensional NMR experiment in conjunction with ^{1}H-detection under fast MAS conditions. This approach has been especially fruitful in the case of studying biomolecules[18–20] and more importantly does not require any special treatment of the sample itself that can lead to structure alternations and in addition only a minuscule amount of sample (a couple of milligrams) is required. However, thus far this approach has not yet been employed in order to attempt to elucidate the structure of the surface species present on heterogeneous catalysts.

Here we present the use of multidimensional ^{1}H-detected ssNMR experiments at high spinning rates in conjunction with computational studies to identify surface sites using supported vanadium compounds prepared via surface organometallic chemistry as a prototypical example since they are an important precursor to model supported vanadium oxide catalysts used in a broad range of applications[21–24] and since their structure is still debated in the literature.[25,26] In this work, we demonstrate how proton-detected ssNMR spectroscopy enables to acquiring high quality NMR spectra for low-abundant (<1%) surface species without the need of labelling. As showcase example, we will focus on elucidating the local environment of grafted vanadium species.[27]

We thus first prepared supported V(V) species via SOMC by grafting $VO(OiPr)_3$ on partially dehydroxylated silica at 700°C that contains mostly isolated OH groups.[28] Figure 1 shows the general scheme and the potential structures that are formed after grafting the precursor on dehydroxylated silica.

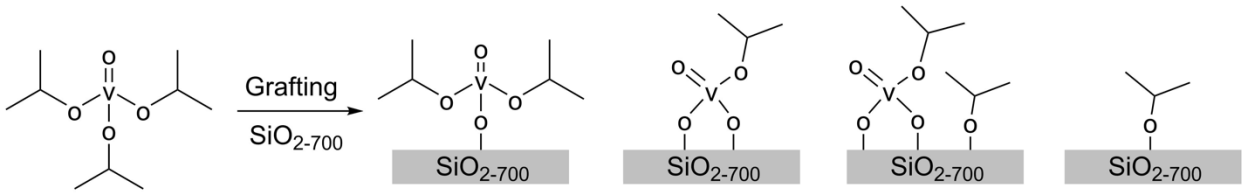

Figure 1. Potential structures formed after grafting $VO(OiPr)_3$ upon silica dehydroxylated at 700°C.

Results of elemental analysis revealed an approximate ratio of 5.5 to 1 Carbon/Vanadium consistent with the loss of ca. 1 isopropoxide ligand upon grafting. The IR spectra shown in Figure S1 before and after grafting clearly show a consumption of isolated surface silanols after grafting with the concomitant appearance of C-H vibrations and a broad OH band after grafting, consistent with the presence of organic ligands and their interaction with residual OH groups (Figure S1).

A ^{1}H NMR spectrum acquired on a 700MHz spectrometer using a 1.3mm rotor and a spinning rate of 50kHz (Figure 2A) shows detailed features that were not observed in previous studies due to the poorer resolution resulting from the use of typical, albeit low rotor spinning rates (ca. 10 kHz)[29]. Overall 4 distinct signals can be identified, two signals at 1.7 and 2.1 ppm that are most likely due to two different types of methyl environments and two signals at 4.9 and 6.2 ppm that can be associated to two inequivalent methine groups of the propyl ligand in very different chemical environment. The ^{51}V NMR spectrum (Figure 2B) recorded under the same conditions shows a single broad signal at -655 ppm, consistent with the formation of one type of V environment. No additional signal at -630 ppm is observed, consistent with the absence of remaining physisorbed molecular precursor. We then further analyzed this sample by correlation spectroscopy in view of the greatly improved resolution and sensitivity gained on the ^{1}H spectrum under these fast MAS conditions. A 2D DQ-SQ 1H-1H correlation spectrum was acquired within

a couple of hours using a single rotor period of recoupling using the BABA sequence[30] (Figure 2C), where the signals around 2 ppm show a correlation with 4 ppm in the indirect dimension and can be therefore be attributed with its self-correlation that can therefore be assigned the methyl groups. The signals at 4.9 and 6.2 ppm do not show self-correlations, consistent with their attribution to –CH methine groups. The improved resolution at these fast MAS rates also allows specific correlations between the –CH and each methyl group to be identified, namely the signals at 6.2 and 4.9 ppm correlates with these at 2.1 and 1.7 ppm, respectively. This result confirms the existence of at least two types of surface OiPr group formed upon grafting $VO(OiPr)_3$ on partially dehydroxylated silica in contrast to what is typically observed for other complexes, where single species are identified.[31]

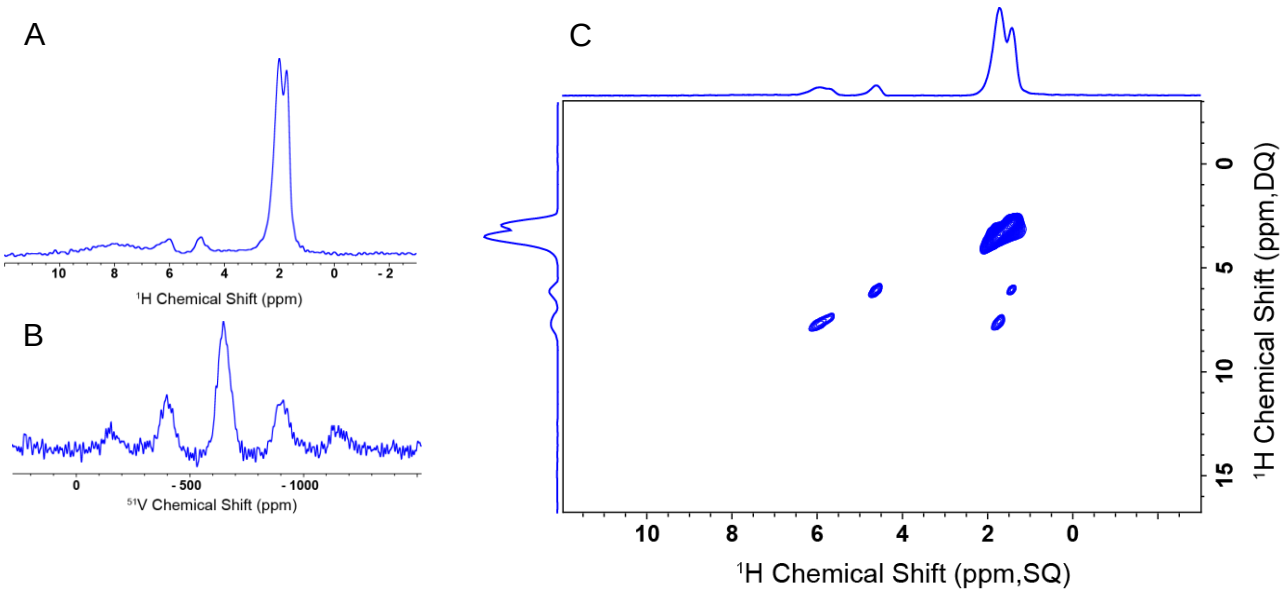

Figure 2. Solid-State NMR spectra recorded on a 700 MHz spectrometer using a 1.3mm probe at 50 kHz MAS. A) and B) show the 1D NMR spectra of ^{1}H and ^{51}V, and C) shows the 2D DQ-SQ ^{1}H-^{1}H NMR spectra recorded of the grafted complex

We thus decided to gain additional structural information through heteronuclear experiments. However, recording ^{13}C spectra or even more so correlation spectra in the absence of isotope enrichment with such small sample volume is typically not undertaken and has mostly been recently possible by using Dynamic Nuclear Polarization Surface Enhanced NMR spectroscopy.[8,9,32–34] However, we show here that the development of ^{1}H detected experiments allows significantly boosting the spectral sensitivity, hence enabling various multidimensional experiments to be performed. In Figure 3A we show a ^{1}H detected heteronuclear ^{1}H-^{13}C spectrum acquired with the D-HMQC[35,36] sequence. The indirect dimension provides direct access to the ^{13}C resonances at 23, 67 and 85 ppm, that can be attributed to having two different isopropoxide species. The ^{13}C chemical shift at 23 ppm correlates with the ^{1}H chemical shift at 1.7 and 2.1 ppm, consistent with their attribution to methyl groups of the isopropyl ligands in different environments. The ^{13}C chemical shifts at 67 and 85 ppm correlate with the ^{1}H resonances at 4.9 and 6.2 ppm, respectively, that can be attributed to inequivalent methine protons and carbons of the propyl ligand, hence the attribution of the signals at 67 and 85 ppm to two inequivalent methine carbons. This significant difference of chemical shift difference further confirms the existence of iPrO surface species in very different chemical environment. Hereby we would also like pointing out that acquiring such a 2D correlation spectra took around 12 hours while previous reported 1D ^{13}C spectra had been acquired in a day with a substantial higher amount of sample. In order to further investigate the structures formed we performed a ^{1}H-^{51}V correlation experiment using the same D-HMQC sequence shown in Figure 3B. The indirect dimension shows a ^{51}V chemical shift of -655 ppm similar to what was observed in the 1D ^{51}V spectrum in Figure 2B. The direct dimension reveals correlations with specific ^{1}H signals, at 2.1 and 6.2 ppm, supporting the attribution of these signals to an isopropoxy ligand bonded to vanadium. The absence of additional

correlations at 1.7 and 4.9 ppm support the attribution of the other isopropoxy ligand to be bound to a silicon rather than vanadium. This interpretation is further supported by the difference of chemical shift since alkoxide ligands bound to d^0 transition-metals are often greatly deshielded,[37,38] because of the presence of low lying empty d orbitals on the metal that modify the electronic structures of bonded ligands.[39] This observation is in line with elemental analysis results which indicated a C:V ratio of 5.5 as mentioned before, thus confirming that approximately 2 isopropoxide ligands remain on the silica surface. Taking together Elemental Analysis results along with the 2D NMR data (that shows an isopropoxide ligand being on the support) we can rule out that the "single site" mono-grafted structure as shown in Figure 1 would be the predominant species on the surfaces and thus a "bis-grafted type" species, formed by grafting and opening of adjacent siloxane bridge, would be more likely.

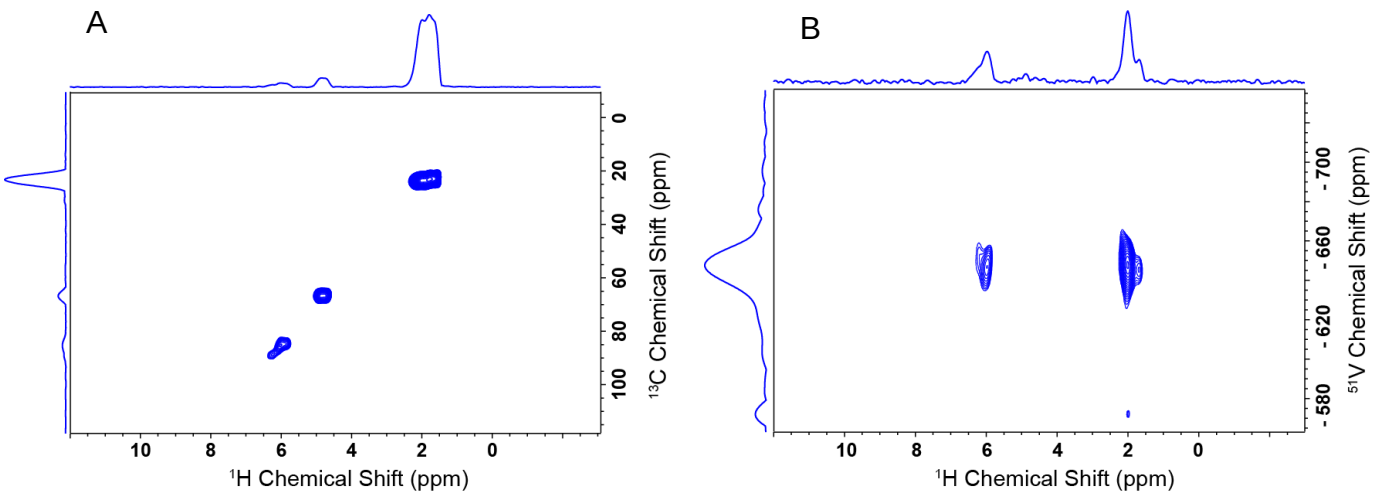

Figure 3. Solid-State NMR spectra recorded on a 700 MHz spectrometer using a 1.3mm probe at 50 kHz MAS. 2D ^{1}H-detected ssNMR spectra recorded with D-HMQC with in A) 2D ^{1}H-^{13}C and in B) a 2D ^{1}H-^{51}V correlation spectra.

In order to further investigate the nature of the surface species present upon grafting on the dehydroxylate silica surface, we complemented our study by using periodic DFT calculations using the VASP[40,41] software package. For the dehydroxylated silica surface we made use of a previously reported model for the silica surface containing 1.1 OH/nm^2 [42] upon which the various grafted V surface structures could be calculated. The structures obtained after geometry optimization are shown in Figure S2 and the calculated NMR parameters of these structures are compared to the experimental ones as shown in Table 1. The calculated chemical shifts for the proton/carbon atoms of the OiPr bound to Si of a dehydroxylated silica surface are 17.7/1.6 and 69.9/5.4 ppm for the methyl and the methine, respectively. In contrast, the calculated chemical shifts for the proton/carbon atoms of the OiPr bound to vanadium ranges between 19.0-21.8/1.4-3.2 and 90.8-94.1/5.6-7.7 ppm for the methyl and the methine, respectively. While these values confirmed the assignment, it shows that one cannot distinguish the potentially different vanadium species based solely on chemical shift because of the narrow chemical shift range.

	"Single sites"	*"bis-grafted"*	*"Complex of bis-grafted + iPrOSi "*	*"iPrOSi"*	*Experiment*
$C^1\underline{H_3}$	1.4	3.2	3.1	1.6	1.7
			3.7		2.1
$C^1\underline{H}$	5.6	7.7	7.6	5.4	6.2
			7.0		4.9
$^{13}\underline{C}H_3$	19.1	21.0	21.8	17.7	23
			18.7		
$^{13}\underline{C}H$	94.1	90.8	90.9	69.9	85
			71.3		67

Table 1. Calculated chemical shift parameters with VASP.

To further ascertain the structure of the surface species, we performed an 2D 1H-1H correlation experiment with short and long RFDR[43] mixing between the protons, since the resolution and sensitivity we have in this experiment under these conditions is sufficient to elucidate this structure this experiment will affirm the proximity of the signals. In Figure 4 we show in blue the 2D 1H-1H spectra with short RFDR recoupling time, where only signals in close proximity will display cross-peaks. This spectrum reveals essentially similar correlations as previously identified in the DQ-SQ experiment from Figure 3C, confirming the attribution, i.e. the OiPr correlations for on the surface and from the OiPr ligand bound to vanadium. However, with increasing RFDR recoupling time to 5ms as shown in the red spectra, additional correlations appear that correspond to through space contacts between the OiPr ligands hence allowing us to confirm the presence of a bis-grafted V oxo isopropoxy species in close proximity to an additional OiPr ligand on the surface. This would therefore suggest that grafting of such a complex involves not only the isolated hydroxide group present on dehydroxylated silica, but also a reactive siloxane bridge in close proximity to vanadium (Figure 5).[44–46]

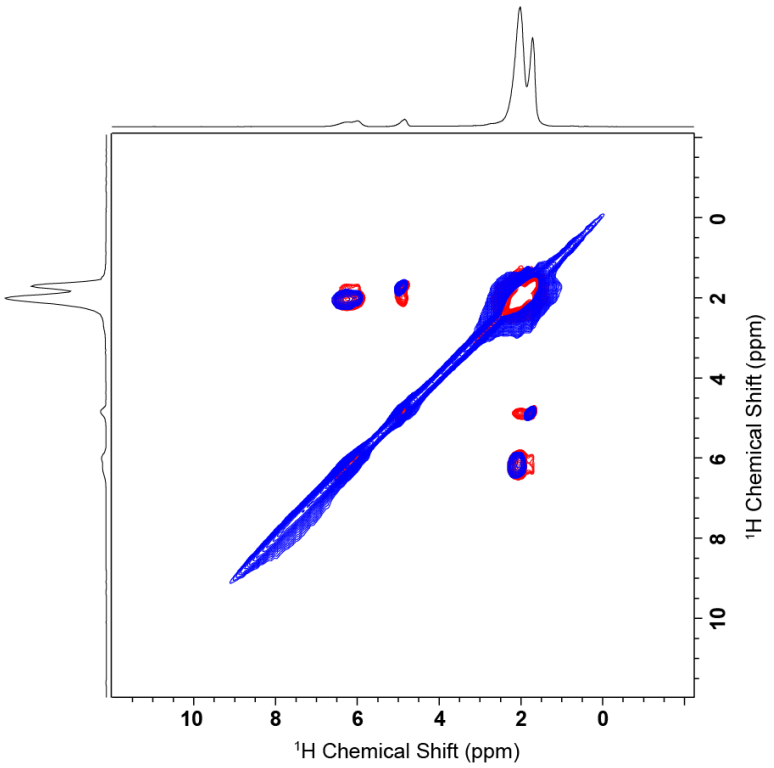

Figure 4. 2D ^{1}H-^{1}H Solid-State NMR spectra recorded on a 700 MHz spectrometer using a 1.3mm probe at 50 kHz MAS with in blue 0.5 ms and in red 5 ms RFDR recoupling.

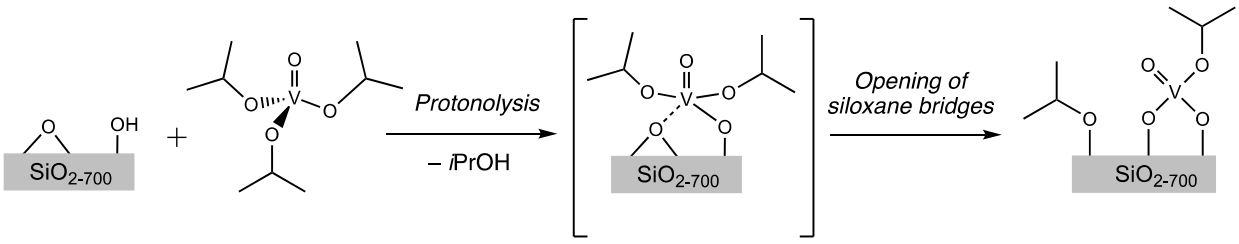

Figure 5. Proposed grafting scheme of $VO(OiPr)_3$ on partially dehydroxylated silica

In conclusion, we have shown how fast MAS ssNMR probes allows the efficient detection of well resolved ^{1}H detected spectra for heterogeneous catalysts. We applied this approach to study the grafting of $VO(OiPr)_3$ using the surface organometallic chemistry method. By exploiting the ^{1}H sensitivity we were able to detect various hetero- and homo-nuclear correlation spectra that provide detailed insight with regards to the structure of the grafted surface species in a time-efficient manner without having to resort to isotope enrichment. In addition, combining this approach with

computational methods greatly aids the interpretation and design of experiments for structural investigations. Our experiments allowed us to resolve the structure of the grafted vanadium complex and show that, in contrast to most other supported metal alkoxides, V grafts via both protonolysis and subsequent opening of adjacent siloxane bridges. We think that our approach will have a beneficial impact on the use of solid-state NMR spectroscopy for studying low abundant surface species due to not having the need to prepare the labelled sample nor needing large sample quantities. Typically, a few mg would suffice meaning that even resorting to isotope enrichment would not lead to a dramatic cost increase, while concurrently greatly aiding the spectral quality and interpretation.

EXPERIMENTAL METHODS

Silica (Aerosil Degussa, 200 m^2g^{-1}) was calcined at 500 °C under air for 12 h and treated under vacuum (10^{-5} mbar) at 500 °C for 8 h followed by 700 °C for 14 h (referred to as $SiO_{2\text{-}700}$)[31] and stored in a glovebox (<0.5ppm H_2O and O_2). Vanadium oxytriisopropoxide, $VO(O^iPr)_3$, was obtained from Sigma-Aldrich and distilled twice until colourless before use. Grafting of $VO(O^iPr)_3$ was performed in benzene onto which 1.5 equivalence based on the silanol content was deposited onto 200mg of thermally pre-treated silica. Subsequently this material was dried under high vacuum and stored inside a glovebox

All experiments were carried out at 16.45 T static magnetic field (700 MHz ^1H frequency) and 50 kHz MAS. The sample temperature was kept at room temperature. Decoupling was performed with the SPINAL64[47] scheme during all direct and indirect acquisition periods. For all experiments and all nuclei, the decoupling amplitude was set to 83kHz.

Periodic ab-initio DFT (Density Functional Theory) calculations were performed with the VASP (Vienna Ab initio Simulation Package)[40,41] software package using the plane-wave pseudopotential method. The GGA (generalized gradient approximation) exchange-correlation

functional of Perdew, Burke and Ernzerhof (PBE)[48] with corrections of dispersion forces from the Grimme approach (DFT + D2)[49] was employed in these calculations. The cutoff energy for the planewave basis set was set to 400eV along with a convergence criterion for the self-consistent field relaxation of 10^{-5}eV. For the geometry optimizations a value of 0.01eV•$Å^{-1}$ was set as the convergence criterion for the conjugate-gradient algorithm. For the silica surface a SiO_2 model[42] was used onto which the molecular precursor would be modelled on. The thickness of the SiO_2 surface was ca 14Å, after including a 20Å vacuum slab the resulting unit cell was 21.39 x 21.39 x 34.2 Å (containing 372 atoms) onto which the structures formed upon grafting have been investigated.

ACKNOWLEDGMENT

D.M. acknowledge support from the ETHZ Postdoctoral Fellowship Program and from the Marie Curie Actions for People COFUND Program. The authors thank I. Moroz for preparing the sample. A. C. V. thanks the Spanish MEC and the European Social Fund for the Ramon y Cajal fellowship (RyC-2016-19930).

REFERENCES

(1) Centi, G.; Perathoner, S. Catalysis and Sustainable (Green) Chemistry. *Catal. Today* **2003**, *77* (4), 287–297. https://doi.org/10.1016/S0920-5861(02)00374-7.

(2) Clark, J. H.; Macquarrie, D. J. Heterogeneous Catalysis in Liquid Phase Transformations of Importance in the Industrial Preparation of Fine Chemicals. *Org. Process Res. Dev.* **1997**, *1* (2), 149–162. https://doi.org/10.1021/op960008m.

(3) Wang, Y.; Wang, X.; Antonietti, M. Polymeric Graphitic Carbon Nitride as a Heterogeneous Organocatalyst: From Photochemistry to Multipurpose Catalysis to Sustainable Chemistry. *Angew. Chemie - Int. Ed.* **2012**, *51* (1), 68–89. https://doi.org/10.1002/anie.201101182.

(4) Carrero, C. A.; Schloegl, R.; Wachs, I. E.; Schomaecker, R. Critical Literature Review of the Kinetics for the Oxidative Dehydrogenation of Propane over Well-Defined Supported Vanadium Oxide Catalysts. *ACS Catal.* **2014**, *4* (10), 3357–3380. https://doi.org/10.1021/cs5003417.

(5) Bañares, M. A.; Wachs, I. E. Molecular Structures of Supported Metal Oxide Catalysts under Different Environments. *J. Raman Spectrosc.* **2002**, *33* (5), 359–380. https://doi.org/10.1002/jrs.866.

(6) Skovpin, I. V.; Zhivonitko, V. V.; Koptyug, I. V. Parahydrogen-Induced Polarization in Heterogeneous Hydrogenations over Silica-Immobilized Rh Complexes. *Appl. Magn. Reson.* **2011**, *41* (2–4), 393–410. https://doi.org/10.1007/s00723-011-0255-z.

(7) Chalupka, K.; Thomas, C.; Millot, Y.; Averseng, F.; Dzwigaj, S. Mononuclear Pseudo-

Tetrahedral V Species of VSiBEA Zeolite as the Active Sites of the Selective Oxidative Dehydrogenation of Propane. *J. Catal.* **2013**, *305*, 46–55. https://doi.org/10.1016/J.JCAT.2013.04.020.

(8) Rossini, A. J.; Zagdoun, A.; Lelli, M.; Lesage, A.; Copéret, C.; Emsley, L. Dynamic Nuclear Polarization Surface Enhanced NMR Spectroscopy. *Acc. Chem. Res.* **2013**, *46* (9), 1942–1951. https://doi.org/10.1021/ar300322x.

(9) Kobayashi, T.; Perras, F. A.; Slowing, I. I.; Sadow, A. D.; Pruski, M. Dynamic Nuclear Polarization Solid-State NMR in Heterogeneous Catalysis Research. *ACS Catal.* **2015**, *5* (12), 7055–7062. https://doi.org/10.1021/acscatal.5b02039.

(10) Mance, D.; van der Zwan, J.; Velthoen, M. E. Z.; Meirer, F.; Weckhuysen, B. M.; Baldus, M.; Vogt, E. T. C. A DNP-Supported Solid-State NMR Study of Carbon Species in Fluid Catalytic Cracking Catalysts. *Chem. Commun.* **2017**, *53* (28), 3933–3936. https://doi.org/10.1039/C7CC00849J.

(11) Wisser, D.; Karthikeyan, G.; Lund, A.; Casano, G.; Karoui, H.; Yulikov, M.; Menzildjian, G.; Pinon, A. C.; Purea, A.; Engelke, F.; et al. BDPA-Nitroxide Biradicals Tailored for Efficient Dynamic Nuclear Polarization Enhanced Solid-State NMR at Magnetic Fields up to 21.1 T. *J. Am. Chem. Soc.* **2018**, *140* (41), 13340–13349. https://doi.org/10.1021/jacs.8b08081.

(12) Liao, W.-C.; Ong, T.-C.; Gajan, D.; Bernada, F.; Sauvée, C.; Yulikov, M.; Pucino, M.; Schowner, R.; Schwarzwälder, M.; Buchmeiser, M. R.; et al. Dendritic Polarizing Agents for DNP SENS. *Chem. Sci.* **2017**, *8* (1), 416–422. https://doi.org/10.1039/C6SC03139K.

(13) Perras, F. A.; Wang, L.-L.; Manzano, J. S.; Chaudhary, U.; Opembe, N. N.; Johnson, D. D.; Slowing, I. I.; Pruski, M. Optimal Sample Formulations for DNP SENS: The Importance of Radical-Surface Interactions. *Curr. Opin. Colloid Interface Sci.* **2018**, *33*, 9–18. https://doi.org/10.1016/J.COCIS.2017.11.002.

(14) Liao, W.-C.; Ghaffari, B.; Gordon, C. P.; Xu, J.; Copéret, C. Dynamic Nuclear Polarization Surface Enhanced NMR Spectroscopy (DNP SENS): Principles, Protocols, and Practice. *Curr. Opin. Colloid Interface Sci.* **2018**, *33*, 63–71. https://doi.org/10.1016/J.COCIS.2018.02.006.

(15) Sangodkar, R. P.; Smith, B. J.; Gajan, D.; Rossini, A. J.; Roberts, L. R.; Funkhouser, G. P.; Lesage, A.; Emsley, L.; Chmelka, B. F. Influences of Dilute Organic Adsorbates on the Hydration of Low-Surface-Area Silicates. *J. Am. Chem. Soc.* **2015**, *137* (25), 8096–8112. https://doi.org/10.1021/jacs.5b00622.

(16) Mathies, G.; Caporini, M. A.; Michaelis, V. K.; Liu, Y.; Hu, K. N.; Mance, D.; Zweier, J. L.; Rosay, M.; Baldus, M.; Griffin, R. G. Efficient Dynamic Nuclear Polarization at 800 MHz/527 GHz with Trityl-Nitroxide Biradicals. *Angew. Chemie - Int. Ed.* **2015**, *54* (40), 11770–11774. https://doi.org/10.1002/anie.201504292.

(17) Jantschke, A.; Koers, E.; Mance, D.; Weingarth, M.; Brunner, E.; Baldus, M. Insight into the Supramolecular Architecture of Intact Diatom Biosilica from DNP-Supported Solid-State NMR Spectroscopy. *Angew. Chemie Int. Ed.* **2015**, *54* (50), 15069–15073. https://doi.org/10.1002/anie.201507327.

(18) Mance, D.; Sinnige, T.; Kaplan, M.; Narasimhan, S.; Daniëls, M.; Houben, K.; Baldus, M.; Weingarth, M. An Efficient Labelling Approach to Harness Backbone and Side-Chain

Protons in 1H-Detected Solid-State NMR Spectroscopy. *Angew. Chemie - Int. Ed.* **2015**, *54* (52), 15799–15803. https://doi.org/10.1002/anie.201509170.

(19) Schanda, P.; Meier, B. H.; Ernst, M. Quantitative Analysis of Protein Backbone Dynamics in Microcrystalline Ubiquitin by Solid-State NMR Spectroscopy. *J. Am. Chem. Soc.* **2010**, *132* (45), 15957–15967. https://doi.org/10.1021/ja100726a.

(20) Linser, R.; Dasari, M.; Hiller, M.; Higman, V.; Fink, U.; Lopez del Amo, J.-M.; Markovic, S.; Handel, L.; Kessler, B.; Schmieder, P.; et al. Proton-Detected Solid-State NMR Spectroscopy of Fibrillar and Membrane Proteins. *Angew. Chemie Int. Ed.* **2011**, *50* (19), 4508–4512. https://doi.org/10.1002/anie.201008244.

(21) Dunn, J. P.; Koppula, P. R.; Stenger, H. G.; Wachs, I. E. Oxidation of Sulfur Dioxide to Sulfur Trioxide over Supported Vanadia Catalysts. **1998**, *19*, 103–117.

(22) Nikolov, V.; Klissurski, D.; Anastasov, A. Phthalic Anhydride from *o* -Xylene Catalysis: Science and Engineering. *Catal. Rev.* **1991**, *33* (3–4), 319–374. https://doi.org/10.1080/01614949108020303.

(23) Nieto, J. M. L.; Concepcion, P.; Dejoz, a; Knozinger, H.; Melo, F.; Vazquez, M. I. Selective Oxidation of N-Butane and Butenes over Vanadium-Containing Catalysts. *J. Catal.* **2000**, *189* (1), 147–157. https://doi.org/10.1006/jcat.1999.2689.

(24) Wada, K.; Yamada, H.; Watanabe, Y.; Mitsudo, T. Selective Photo-Assisted Catalytic Oxidation of Methane and Ethane to Oxygenates Using Supported Vanadium Oxide Catalysts. **1998**, *2* (12), 1771–1778.

(25) Love, A. M.; Carrero, C. A.; Chieregato, A.; Grant, J. T.; Conrad, S.; Verel, R.; Hermans,

I. Elucidation of Anchoring and Restructuring Steps during Synthesis of Silica-Supported Vanadium Oxide Catalysts. *Chem. Mater.* **2016**, *28* (15), 5495–5504. https://doi.org/10.1021/acs.chemmater.6b02118.

(26) H, M. P.; Min Serena Goh, L.; Abou-Hamad, E.; Barman, S.; Dachwald, O.; Ahmad Pasha, F.; Pelletier, J.; Cavallo, L.; Basset, J.-M. SOMC Grafting of Vanadium Oxytriisopropoxide (VO(OiPr)3) on Dehydroxylated Silica Analysis of Surface Complexes and Thermal Restructuring Mechanism. **2018**. https://doi.org/10.1039/c8ra02419g.

(27) Mance, D.; Copéret, C. Elucidating the Structure of Surface Sites Using 1H-Detected SsNMR Spectroscopy: The Case of Isolated V Oxo Selective Oxidation Catalysts. *60th ENC Conf. April 7-12* **2019**.

(28) Rascón, F.; Wischert, R.; Copéret, C. Molecular Nature of Support Effects in Single-Site Heterogeneous Catalysts: Silica vs. Alumina. *Chem. Sci.* **2011**, *2* (8), 1449. https://doi.org/10.1039/c1sc00073j.

(29) Lesage, A.; Duma, L.; Sakellariou, D.; Emsley, L. Improved Resolution in Proton NMR Spectroscopy of Powdered Solids. **2001**. https://doi.org/10.1021/ja0039740.

(30) Feike, M.; Demco, D. E.; Graf, R.; Gottwald, J.; Hafner, S.; Spiess, H. W. Broadband Multiple-Quantum NMR Spectroscopy. *J. Magn. Reson. Ser. A* **1996**, *122* (2), 214–221. https://doi.org/10.1006/jmra.1996.0197.

(31) Copéret, C.; Comas-Vives, A.; Conley, M. P.; Estes, D. P.; Fedorov, A.; Mougel, V.; Nagae, H.; Núnez-Zarur, F.; Zhizhko, P. A. Surface Organometallic and Coordination Chemistry toward Single-Site Heterogeneous Catalysts: Strategies, Methods, Structures, and

Activities. *Chem. Rev.* **2016**, *116* (2), 323–421. https://doi.org/10.1021/acs.chemrev.5b00373.

(32) Lesage, A.; Lelli, M.; Gajan, D.; Caporini, M. A.; Vitzthum, V.; Miéville, P.; Alauzun, J.; Roussey, A.; Thieuleux, C.; Mehdi, A.; et al. Surface Enhanced NMR Spectroscopy by Dynamic Nuclear Polarization. *J. Am. Chem. Soc.* **2010**, *132* (44), 15459–15461. https://doi.org/10.1021/ja104771z.

(33) Copéret, C.; Liao, W.-C.; Gordon, C. P.; Ong, T.-C. Active Sites in Supported Single-Site Catalysts: An NMR Perspective. *J. Am. Chem. Soc.* **2017**, *139* (31), 10588–10596. https://doi.org/10.1021/jacs.6b12981.

(34) Hu, K.-N.; Yu, H.; Swager, T. M.; Griffin, R. G. Dynamic Nuclear Polarization with Biradicals. *J. Am. Chem. Soc.* **2004**, *126* (35), 10844–10845. https://doi.org/10.1021/ja039749a.

(35) Trebosc, J.; Hu, B.; Amoureux, J. P.; Gan, Z. Through-Space R 3-HETCOR Experiments between Spin-1/2 and Half-Integer Quadrupolar Nuclei in Solid-State NMR. **2007**. https://doi.org/10.1016/j.jmr.2007.02.015.

(36) Gan, Z. C/ 14 N Heteronuclear Multiple-Quantum Correlation with Rotary Resonance and REDOR Dipolar Recoupling. **2006**. https://doi.org/10.1016/j.jmr.2006.09.016.

(37) Alphazan, T.; Mathey, L.; Schwarzwälder, M.; Lin, T.-H.; Rossini, A. J.; Wischert, R.; Enyedi, V.; Fontaine, H.; Veillerot, M.; Lesage, A.; et al. Monolayer Doping of Silicon through Grafting a Tailored Molecular Phosphorus Precursor onto Oxide-Passivated Silicon Surfaces. *Chem. Mater.* **2016**, *28* (11), 3634–3640.

https://doi.org/10.1021/acs.chemmater.5b04291.

(38) Grau, E.; Lesage, A.; Norsic, S.; Copéret, C.; Monteil, V.; Sautet, P. Tetrahydrofuran in TiCl 4 /THF/MgCl 2 : A Non-Innocent Ligand for Supported Ziegler−Natta Polymerization Catalysts. **2012**. https://doi.org/10.1021/cs300764h.

(39) Gordon, C. P.; Raynaud, C.; Andersen, R. A.; Copéret, C.; Eisenstein, O. Carbon-13 NMR Chemical Shift: A Descriptor for Electronic Structure and Reactivity of Organometallic Compounds. *Acc. Chem. Res.* **2019**, *52* (8), 2278–2289. https://doi.org/10.1021/acs.accounts.9b00225.

(40) Kresse, G.; Hafner, J. *Ab Initio* Molecular-Dynamics Simulation of the Liquid-Metal–Amorphous-Semiconductor Transition in Germanium. *Phys. Rev. B* **1994**, *49* (20), 14251–14269. https://doi.org/10.1103/PhysRevB.49.14251.

(41) Kresse, G.; Furthmüller, J. Efficient Iterative Schemes for *Ab Initio* Total-Energy Calculations Using a Plane-Wave Basis Set. *Phys. Rev. B* **1996**, *54* (16), 11169–11186. https://doi.org/10.1103/PhysRevB.54.11169.

(42) Comas-Vives, A. Amorphous SiO $_2$ Surface Models: Energetics of the Dehydroxylation Process, Strain, Ab Initio Atomistic Thermodynamics and IR Spectroscopic Signatures. *Phys. Chem. Chem. Phys.* **2016**, *18* (10), 7475–7482. https://doi.org/10.1039/C6CP00602G.

(43) Bennett, A. E.; Rienstra, C. M.; Griffiths, J. M.; Zhen, W.; Lansbury, P. T.; Griffin, R. G. Homonuclear Radio Frequency-Driven Recoupling in Rotating Solids. *J. Chem. Phys.* **1998**, *108* (22), 9463–9479. https://doi.org/10.1063/1.476420.

(44) Ahn, H.; Marks, T. J. High-Resolution Solid-State 13C NMR Studies of Chemisorbed

Organometallics. Chemisorptive Formation of Cation-like and Alkylidene Organotantalum Complexes on High Surface Area Inorganic Oxides. **2002**. https://doi.org/10.1021/JA0123204.

(45) Roux, E. Le; Chabanas, M.; Baudouin, A.; Mallmann, A.; Copéret, C.; Quadrelli, E. A.; Thivolle-Cazat, J.; Basset, J.-M.; Lukens, W.; Lesage, A.; et al. Detailed Structural Investigation of the Grafting of [Ta(CHtBu)(CH2tBu)3] and [Cp*TaMe4] on Silica Partially Dehydroxylated at 700 °C and the Activity of the Grafted Complexes toward Alkane Metathesis. **2004**. https://doi.org/10.1021/JA046486R.

(46) Rataboul, F.; Baudouin, A.; Thieuleux, C.; Veyre, L.; Copéret, C.; Thivolle-Cazat, J.; Basset, J.-M.; Lesage, A.; Emsley, L. Molecular Understanding of the Formation of Surface Zirconium Hydrides upon Thermal Treatment under Hydrogen of [(≡SiO)Zr(CH2tBu)3] by Using Advanced Solid-State NMR Techniques. **2004**. https://doi.org/10.1021/JA038486H.

(47) Fung, B. M.; Khitrin, A. K.; Ermolaev, K. An Improved Broadband Decoupling Sequence for Liquid Crystals and Solids. *J. Magn. Reson.* **2000**, *142* (1), 97–101. https://doi.org/10.1006/jmre.1999.1896.

(48) Perdew, J.; Burke, K.; Ernzerhof, M. Generalized Gradient Approximation Made Simple. *Phys. Rev. Lett.* **1996**, *77* (18), 3865–3868. https://doi.org/10.1103/PhysRevLett.77.3865.

(49) Grimme, S. Semiempirical GGA-Type Density Functional Constructed with a Long-Range Dispersion Correction. *J. Comput. Chem.* **2006**, *27* (15), 1787–1799. https://doi.org/10.1002/jcc.20495.

Supporting Information

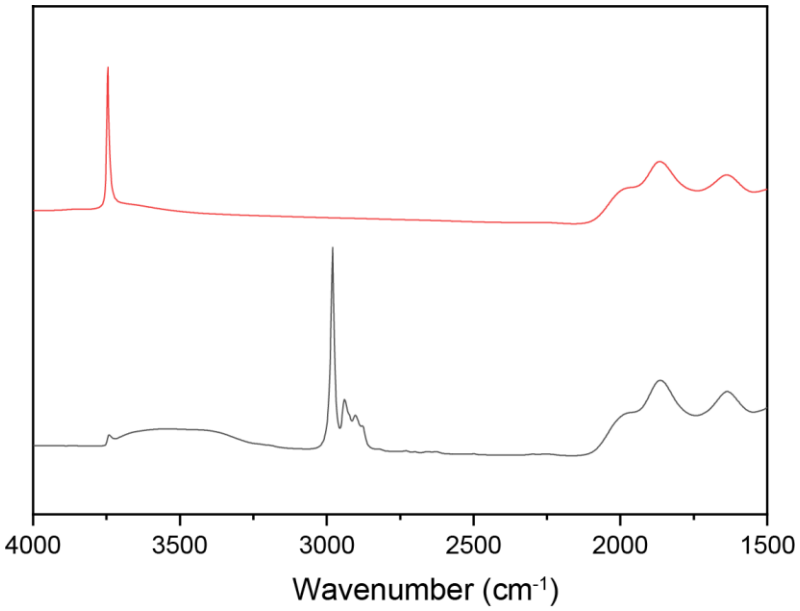

Figure S1. FTIR recorded in transmission mode with in red the spectrum of dehydroxylated silica at 700°C and in black the spectrum after grafting vanadium oxytriisopropoxide onto the dehydroxylated silica

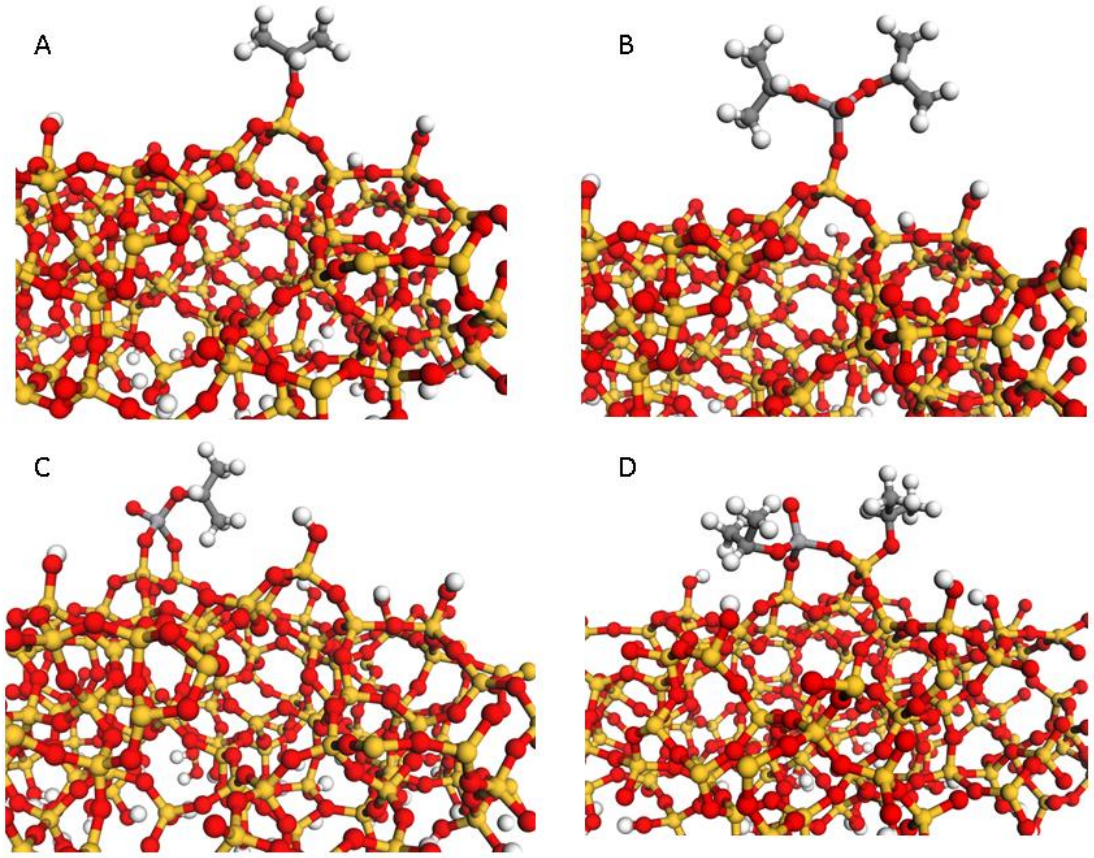

Figure S2. Geometry optimized surface structures using VASP. A) OiPr, B) single sites $VO(OiPr)_2$, C) bis-grafted VO(OiPr) and D) bis-grafted VO(OiPr) within presence of OiPr modeled on dehydroxylated silica.